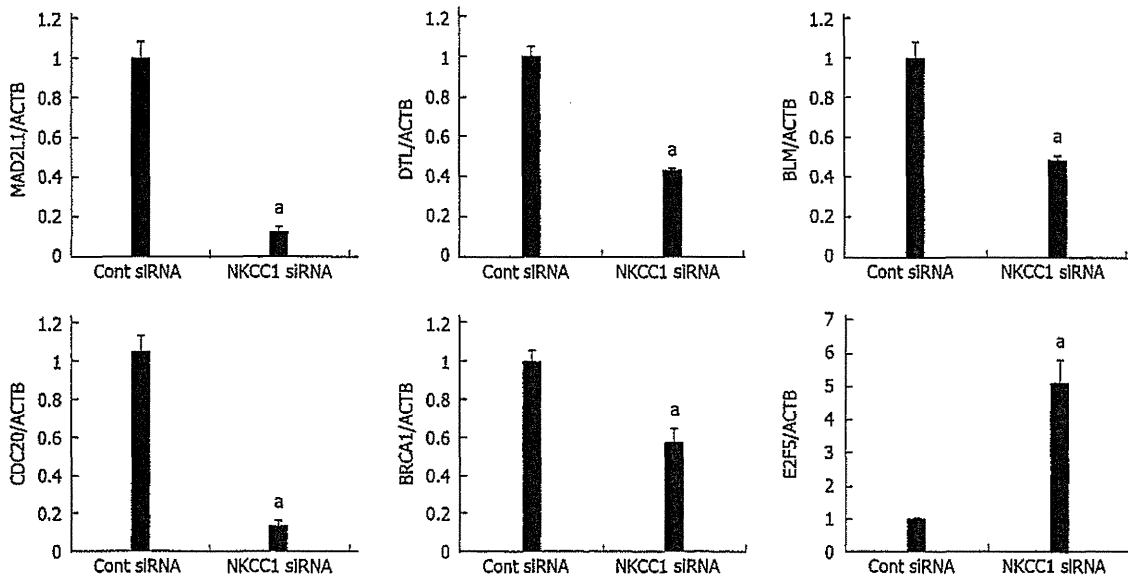
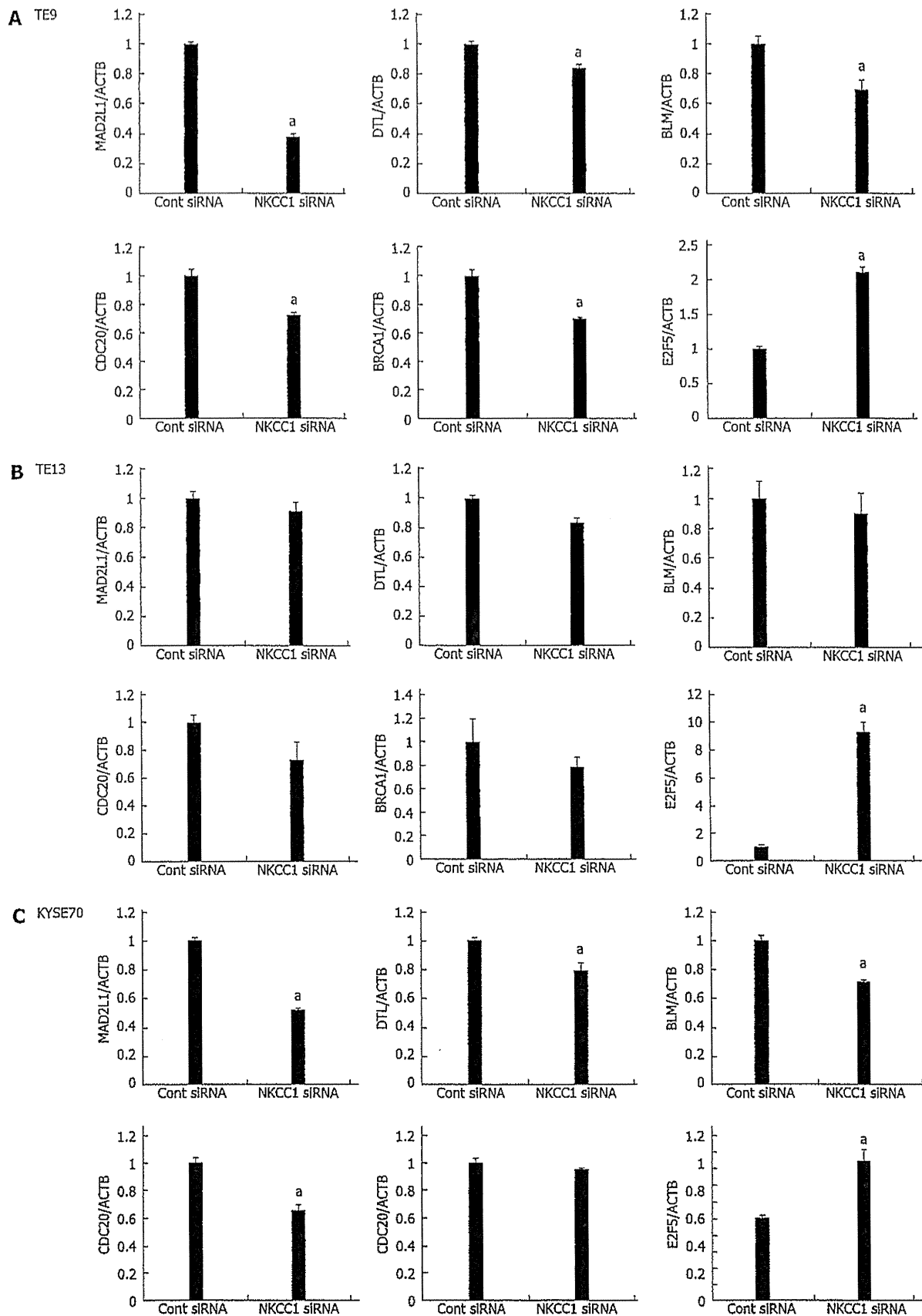


**Figure 5** Top-ranked signaling networks related to Na<sup>+</sup>/K<sup>+</sup>/2Cl<sup>-</sup> cotransporter 1 downregulation according to ingenuity pathway analysis. A: This network is called "Cellular Assembly and Organization; DNA Replication, Recombination, and Repair; Cell Cycle"; B: This network is called "Cellular Assembly and Organization, Cell Cycle, DNA Replication, Recombination, and Repair"; C: This network is called "Cell Cycle; DNA Replication, Recombination, and Repair; Cancer". Red and green indicate genes with expression levels that were higher or lower, respectively, than reference RNA levels. Genes analyzed for verification in Figure 6 were highlighted by red circles.



**Figure 6** Verification of gene expression by real-time quantitative reverse transcription-polymerase chain reaction. The expression levels of six selected genes (MAD2L1, DTL, BLM, CDC20, BRCA1, and E2F5) in NKCC1 depleted KYSE170 cells were compared to those in control siRNA transfected cells using real-time quantitative reverse transcription-polymerase chain reaction. Gene expression levels were normalized to the level of ACTB. The mean  $\pm$  SEM.  $n = 3$ . \* $P < 0.05$  vs control siRNA.



**Figure 7** Expression levels of six selected genes (MAD2L1, DTL, BLM, CDC20, BRCA1, and E2F5) in Na<sup>+</sup>/K<sup>+</sup>/2Cl<sup>-</sup> cotransporter 1 depleted TE9, TE13 and KYSE70 cells. The expression levels of six selected genes (MAD2L1, DTL, BLM, CDC20, BRCA1, and E2F5) in Na<sup>+</sup>/K<sup>+</sup>/2Cl<sup>-</sup> cotransporter 1 (NKCC1) depleted TE9 (A), TE13 (B) and KYSE70 cells (C) were compared to those in control siRNA transfected cells using real-time quantitative RT-PCR. Gene expression levels were normalized to the level of ACTB. The mean ± SEM. *n* = 3. \**P* < 0.05 vs control siRNA.

**Table 3** Top biological functions, canonical pathways, and networks of Na<sup>+</sup>/K<sup>+</sup>/2Cl<sup>-</sup> cotransporter 1 according to Ingenuity Pathway Analysis

Top Biological Functions		
Diseases and disorders		
Name	P value	Number of molecules
Cancer	2.08E-12 - 1.59E-02	277
Gastrointestinal disease	8.03E-12 - 1.60E-02	149
Reproductive system disease	2.25E-09 - 1.57E-02	138
Hematological disease	1.72E-06 - 1.22E-02	70
Hereditary disorder	2.10E-06 - 1.57E-02	120
Molecular and cellular functions		
Name	P value	Number of molecules
Cell cycle	1.06E-20 - 1.60E-02	158
Cellular assembly and organization	1.06E-20 - 1.36E-02	111
DNA replication, recombination, and repair	1.06E-20 - 1.16E-02	133
Cellular movement	8.36E-11 - 1.51E-02	82
Cell death	2.98E-06 - 1.56E-02	216
Top canonical pathways		
Name	P value	Ratio
Role of BRCA1 in the DNA damage response	9.79E-6	12/65 (0.185)
Mitotic roles of Polo-Like kinase	7.37E-5	11/69 (0.159)
Estrogen-mediated S-phase entry	4.91E-4	6/28 (0.214)
Cell Cycle: G2/M DNA damage checkpoint regulation	5.07E-4	8/49 (0.163)
Role of CHK proteins in cell cycle checkpoint control	5.37E-4	9/56 (0.161)
Top networks		
Associated network functions	Score	
Cellular assembly and organization; DNA replication, recombination, and repair; Cell cycle	47	
Cellular assembly and organization, Cell cycle, DNA replication, recombination, and repair	43	
Cell cycle; DNA replication, recombination, and repair; Cancer	37	
Digestive system development and function, organismal injury and abnormalities, cellular function and maintenance	37	
Cellular assembly and organization; DNA replication, recombination, and repair; Cardiovascular disease	35	

was downregulated in NKCC1 depleted KYSE170 cells (fold change: -28.92; Table 2). Ingenuity Pathway Analysis showed that "Cancer" was the top-ranked disease and that "Cell Cycle" was the top-ranked biological function related to NKCC1 depletion. Furthermore, "Cell Cycle: G2/M DNA Damage Checkpoint Regulation" was one of the top-ranked canonical pathways related to NKCC1 depletion (Table 3), and this result was in agreement with the results obtained *via* cell cycle analysis. Among the 2527 genes with expression levels that were altered by NKCC1 depletion, 267 genes exhibited cell proliferation-related functions (Table 4). Among these genes, 82 genes were upregulated, and the other 185 genes were downregulated. We then examined the signal transduction networks induced by NKCC1 depletion (Table 3). All of the top 3 ranked signal networks were related to the cell cycle (Figure 5). These results indicate that the expression level of NKCC1 influences genes related to cellular growth and cell cycle progression.

#### Verification of gene expression by real-time quantitative RT-PCR

Six genes (MAD2L1, DTL, BLM, CDC20, BRCA1, and E2F5) were further examined by quantitative Real time reverse transcription-polymerase chain reaction (RT-PCR). BLM was chosen from Network A, MAD2L1 and

CDC20 from Network B, and DTL and E2F from Network C (Figure 5). BRCA1 was chosen because "Role of BRCA1 in DNA Damage Response" was the top-ranked canonical pathway related to NKCC1 (Table 3). All of these genes were related to the G2/M checkpoint according to IPA and are included in Table 4. The expression levels of MAD2L1, DTL, BLM, CDC20, and BRCA1 mRNA were significantly lower in NKCC1 depleted KYSE170 cells compared to control siRNA transfected cells (Figure 6). The expression levels of E2F5 mRNA were significantly higher in NKCC1 depleted KYSE170 cells compared to control siRNA transfected cells (Figure 6). Similar trends were found in several cell lines, including TE9, TE13 and KYSE 70 which expressed NKCC1 (Figure 7). These changes were in agreement with the microarray results and suggest that NKCC1 controls cell cycle progression *via* G<sub>2</sub>/M checkpoint regulation in ESCC cells.

#### DISCUSSION

The roles of ion transporters have recently been studied in cancer cells<sup>[14,15]</sup>. Some types of K<sup>+</sup> channels have been reported to be expressed at high levels in colonic carcinoma<sup>[16,17]</sup>. The voltage-gated HERG channel has also exhibited cancer-specific expression in gastric can-

**Table 4. Cell growth-related genes with expression levels in KYSE170 cells that were changed by the depletion of Na<sup>+</sup>/K<sup>+</sup>/2Cl<sup>-</sup> cotransporter 1**

Gene symbol	Gene ID	Biological functions		Fold change
		Cell growth and proliferation	Cell cycle	
<b>Upregulated genes</b>				
NDN	NM_002487	•		66.45
INPP5D	NM_001017915	•	•	52.83
CCR1	NM_001295	•		44.86
COL1A2	NM_000089	•		36.72
EDAR	NM_022336	•	•	35.86
RBP4	NM_006744	•		30.40
DCLK1	NM_004734	•	•	28.95
RARRES1	NM_002888	•		22.92
FMOD	NM_002023	•		22.85
BARX1	NM_021570	•		21.47
MAPK10	NM_138980	•		20.00
ADORA2A	NM_000675	•		18.78
CHRNA7	NM_001190455	•	•	18.47
SOX10	NM_006941	•		18.03
FGF20	NM_019851	•		16.73
FAM5C	NM_199051	•	•	14.35
MBD2	NM_015832	•		12.13
EGF	NM_001963	•	•	11.50
TLR5	NM_003268	•		11.35
TNN	NM_022093	•		10.98
SLC1A2	NM_004171	•		10.74
CD36	NM_001001547	•		10.43
CD52	NM_001803	•		10.34
NR2E3	NM_016346	•		10.31
PLCB1	NM_182734	•	•	10.26
MYCN	NM_005378	•	•	10.23
ZNF365	NM_199451	•	•	10.12
ERG	NM_004449	•		10.04
MSH4	NM_002440	•	•	10.03
DMRT1	NM_021951	•		9.61
RNF128	NM_194463	•		9.37
CD69	NM_001781	•		8.89
PDE3A	NM_000921	•	•	8.58
ACVR1C	NM_145259	•		8.57
SPI1	NM_001080547	•	•	8.55
SH2D3C	NM_170600	•		8.53
IFNG	NM_000619	•	•	8.22
MRAS	NM_012219	•		8.20
MCF2L	NM_024979	•		7.43
RRAD	NM_004165	•	•	7.42
E2F5	NM_001951	•	•	7.32
BGN	NM_001711	•		7.13
KIFC1	NM_002263	•	•	7.02
ABCC6	NM_001171	•		6.98
SERPINE1	NM_000602	•		6.74
CHIITA	NM_000246	•		6.74
GJB6	NM_006783	•		6.45
TP53INP1	NM_033285	•	•	6.38
GHRL	NM_016362	•		6.30
CCNG2	NM_004354	•	•	6.29
RORC	NM_005060	•		6.24
NCF1	NM_000265	•		6.24
NFATC4	NM_001136022	•		6.15
CHRM5	NM_012125	•		6.01
HMOX1	NM_002133	•	•	6.00
IL18RAP	NM_003853	•		5.98
C8orf4	NM_020130	•		5.95
L1CAM	NM_024003	•		5.87
TNFSF8	NM_001244	•		5.85
MSMB	NM_002443	•		5.77
ITPR1	NM_002222	•		5.77
ITGAL	NM_002209	•	•	5.73
INHBA	NM_002192	•	•	5.53
HEYL	NM_014571	•		5.38
JAK3	NM_000215	•	•	5.30
MMP13	NM_002427	•		5.23
NNMT	NM_006169	•		5.06
BNIP1	NM_138278	•		4.86
LTC4S	NM_145867	•	•	4.74
MMP24	NM_006690	•		4.72
MMP1	NM_002421	•		4.66
CD19	NM_001770	•	•	4.52
ADC	NM_052998	•		4.46
TGFBRI	NM_004612	•	•	4.33
RHOB	NM_004040	•		4.32
CDKN1C	NM_000076	•	•	4.30
HOXB13	NM_006361	•	•	4.20
IPMK	NM_152230	•		4.07
BMF	NM_001003940	•		4.06
VTCN1	NM_024626	•	•	4.05
CEACAM1	NM_001712	•		2.97
TSSK3	NM_052841	•	•	2.00
<b>Downregulated genes</b>				
CRHR2	NM_001883	•		-39.78
C5	NM_001735	•	•	-39.13
KCNMA1	NM_001014797	•		-38.59
GRIA1	NM_000827	•		-31.27
SLC12A2	NM_001046	•		-28.92
APOA1	NM_000039	•		-25.21
PRKAR2B	NM_002736	•	•	-24.25
TF	NM_001063	•		-22.85
BRCA2	NM_000059	•	•	-22.04
AURKC	NM_001015878	•	•	-21.69
PLXNA4	NM_181775	•		-20.54
TYR	NM_000372	•		-20.39
BACH2	NM_021813	•		-20.01
KIF14	NM_014875	•	•	-18.06
HEY2	NM_012259	•		-18.01
TMPO	NM_003276	•	•	-15.97
FCGR3A	NM_000569	•		-15.18
ARF6	NM_001663	•		-15.09
MYBL1	NM_001080416	•	•	-14.60
CCNA1	NM_003914	•	•	-14.29
ESCO2	NM_001017420	•	•	-14.05
TOP2A	NM_001067	•		-13.91
CENPI	NM_006733	•	•	-13.87
ATAD2	NM_014109	•		-13.41
POSTN	NM_006475	•		-12.91
MKI67	NM_002417	•	•	-12.41
ABCB1	NM_000927	•		-12.15
KIF20B	NM_016195	•	•	-11.53
SPN	NM_001030288	•		-11.41
MAD2L1	NM_002358	•	•	-11.16
HLA-DPB1	NM_002121	•		-11.12
SGOL1	NM_001012410	•	•	-10.91
RRM2	NM_001034	•		-10.71
FANCD2	NM_033084	•	•	-10.55
FANCA	NM_001018112	•	•	-10.31
HDAC2	NM_001527	•	•	-9.94
NUF2	NM_145697	•	•	-9.76
CLSPN	NM_022111	•	•	-9.57
RAD54L	NM_003579	•		-9.47
KLHL13	NM_033495	•	•	-9.32
CCNA2	NM_001237	•	•	-9.13
MCM10	NM_182751	•	•	-9.11
MCTS1	NM_014060	•		-9.02
ANLN	NM_018685	•	•	-9.00
HMGB2	NM_002129	•	•	-8.86
VPREB1	NM_007128	•		-8.81
KIF4A	NM_012310	•	•	-8.78
SPC25	NM_020675	•		-8.75
ALOX5	NM_000698	•	•	-8.55

PBK	NM_018492	•	-8.20	PNN	NM_002687	•	•	-5.20
TNFRSF11B	NM_002546	•	-8.20	NTRK3	NM_001007156	•	•	-5.17
CIT	NM_001206999	•	-8.17	IL25	NM_022789	•	•	-5.09
HELLS	NM_018063	•	-8.1	UBE2C	NM_181803	•	•	-5.09
CDC45	NM_003504	•	-8.07	AURKB	NM_004217	•	•	-5.08
DTL	NM_016448	•	-8.00	CDC6	NM_001254	•	•	-5.08
RGS3	NM_017790	•	-7.93	CDKN2C	NM_078626	•	•	-5.06
TYMS	NM_001071	•	-7.87	EDN2	NM_001956	•	•	-5.06
NDC80	NM_006101	•	-7.86	CDC20	NM_001255	•	•	-5.05
ERCC6L	NM_017669	•	-7.82	RRM1	NM_001033	•	•	-5.05
CENPE	NM_001813	•	-7.75	APC	NM_000038	•	•	-5.04
TTK	NM_003318	•	-7.74	KIF15	NM_020242	•	•	-5.03
SIM2	NM_009586	•	-7.61	LMNB1	NM_005573	•	•	-5.02
KRT4	NM_002272	•	-7.55	NCAPG2	NM_017760	•	•	-4.96
RAD51AP1	NM_006479	•	-7.55	CCNE2	NM_057749	•	•	-4.94
LTA	NM_000595	•	-7.51	HMMR	NM_012484	•	•	-4.93
PAK2	NM_002577	•	-7.50	BRIP1	NM_032043	•	•	-4.90
SLCSA8	NM_145913	•	-7.41	ECT2	NM_018098	•	•	-4.89
BLM	NM_000057	•	-7.40	CDT1	NM_030928	•	•	-4.87
NUSAP1	NM_016359	•	-7.36	MCAM	NM_006500	•	•	-4.82
JDP2	NM_130469	•	-7.19	LAG3	NM_002286	•	•	-4.78
CASP3	NM_004346	•	-7.17	ZWINT	NM_032997	•	•	-4.73
NEIL3	NM_018248	•	-7.17	DCLK2	NM_001040260	•	•	-4.72
POLH	NM_006502	•	-7.11	TRAP	NM_005879	•	•	-4.71
KIF20A	NM_005733	•	-7.08	SSTR2	NM_001050	•	•	-4.69
MYO7A	NM_000260	•	-6.93	TXK	NM_003328	•	•	-4.65
NRGN	NM_006176	•	-6.82	TBC1D9	NM_015130	•	•	-4.63
NCAPG	NM_022346	•	-6.78	IL1RN	NM_173843	•	•	-4.61
CDCA8	NM_018101	•	-6.72	CDCA7	NM_031942	•	•	-4.56
CEP55	NM_018131	•	-6.65	STK38	NM_007271	•	•	-4.56
DLGAP5	NM_014750	•	-6.60	CDCA5	NM_080668	•	•	-4.54
CDC25C	NM_001790	•	-6.59	E2F7	NM_203394	•	•	-4.54
ARL2BP	NM_012106	•	-6.58	FIGNL1	NM_001042762	•	•	-4.51
IL12A	NM_000882	•	-6.53	SMC4	NM_005496	•	•	-4.50
MYH14	NM_001077186	•	-6.52	CYCS	NM_018947	•	•	-4.48
SKA1	NM_001039535	•	-6.46	FBN1	NM_000138	•	•	-4.48
CASC1	NM_018272	•	-6.44	NCAPD3	NM_015261	•	•	-4.46
HJURP	NM_018410	•	-6.42	IL16	NM_172217	•	•	-4.44
TACC3	NM_006342	•	-6.33	PCNA	NM_002592	•	•	-4.42
ENPP3	NM_005021	•	-6.30	FBXO5	NM_001142522	•	•	-4.37
STIL	NM_001048166	•	-6.27	CKAP2	NM_018204	•	•	-4.34
KNTC1	NM_014708	•	-6.26	IL34	NM_152456	•	•	-4.34
NR1I2	NM_003889	•	-6.24	PSRC1	NM_032636	•	•	-4.33
AKR1B10	NM_020299	•	-6.22	C11orf82	NM_145018	•	•	-4.32
E2F2	NM_004091	•	-6.20	CHRDL1	NM_145234	•	•	-4.31
USP47	NM_017944	•	-6.14	RAD54B	NM_012415	•	•	-4.31
KIF11	NM_004523	•	-6.09	DIAPH3	NM_001042517	•	•	-4.29
E2F8	NM_024680	•	-6.05	AKR1C1	NM_001353	•	•	-4.26
PLK1	NM_005030	•	-6.02	INHBB	NM_002193	•	•	-4.25
CCDC6	NM_005436	•	-6.00	MDM2	NM_002392	•	•	-4.25
ORC6	NM_014321	•	-6.00	PRKAA1	NM_206907	•	•	-4.25
EXO1	NM_003686	•	-5.95	MASTL	NM_032844	•	•	-4.23
GFC5	NM_004466	•	-5.94	MCM5	NM_006739	•	•	-4.21
GSG2	NM_031965	•	-5.93	CD2AP	NM_012120	•	•	-4.20
PRC1	NM_003981	•	-5.89	BRC1	NM_007300	•	•	-4.18
RAD51	NM_002875	•	-5.78	TPX2	NM_012112	•	•	-4.15
KIF2C	NM_006845	•	-5.71	FGFBP1	NM_005130	•	•	-4.14
TNFRSF13C	NM_052945	•	-5.70	EIF4G2	NM_001172705	•	•	-4.12
BLZF1	NM_003666	•	-5.63	AURKA	NM_198433	•	•	-4.10
FEN1	NM_004111	•	-5.51	PTTG1	NM_004219	•	•	-4.08
PLK4	NM_014264	•	-5.49	ADRA1B	NM_000679	•	•	-4.07
HAS2	NM_005328	•	-5.44	RECQL4	NM_004260	•	•	-4.02
PKMYT1	NM_182687	•	-5.40	GJB2	NM_004004	•	•	-4.00
BUB1	NM_001211	•	-5.34	BIRC5	NM_001012271	•	•	-3.35
BUB1B	NM_001211	•	-5.34	TERF1	NM_017489	•	•	-3.18
NEK2	NM_002497	•	-5.33	LRP1	NM_032832	•	•	-2.43
IQGAP3	NM_178229	•	-5.27	CDK1	NM_012395	•	•	-2.21
SKA3	NM_145061	•	-5.23	ARHGEF10	NM_014629	•	•	-2.08

cer and its blocker diminished the G<sub>1</sub> to S phase transition<sup>[18]</sup>. Increased mRNA levels of Ca<sup>2+</sup> channels have also been reported in colorectal adenocarcinoma<sup>[19,20]</sup>. Furthermore, some reports have indicated that Cl<sup>-</sup> channels/transporters, such as Cl<sup>-</sup> channels, K<sup>+</sup>/Cl<sup>-</sup> cotransporters, and NKCC play important roles in the proliferation of colorectal, breast, lung, and prostate cancer cells<sup>[14,15]</sup>. To the best of our knowledge, the present study is the first report examining NKCC1 expression in ESCC tissue and the gene expression profile of NKCC1 depleted cancer cells.

We investigated the role of transepithelial Cl<sup>-</sup> transport in cancer cells<sup>[5-7]</sup>. In the present study, we found that the depletion of NKCC1 induced G<sub>2</sub>/M phase arrest in KYSE170 cells. We have previously shown that the blockage of NKCC inhibited G<sub>1</sub>/S cell cycle progression in gastric and prostate cancer cells<sup>[8,9]</sup>, which suggests that the mechanism by which NKCC1 regulates cell cycle progression varies among cell types and their different genetic backgrounds. Microarray analysis showed that many of the genes that displayed changes in expression levels after NKCC1 depletion were well connected in the top-ranked signaling network related to the cell cycle, indicating that they are not only functionally related but are also regulated together at the level of expression by NKCC1-related signal transduction pathways.

With regard to signaling networks, we noted that the expression levels of several G<sub>2</sub>/M checkpoint-related genes were altered by the depletion of NKCC1. In the spindle checkpoint, the anaphase-promoting complex (APC) was activated by CDC20, which subsequently triggered anaphase. MAD2L1, a mitotic spindle assembly checkpoint protein, inhibited the activity of the APC by a direct physical interaction with a ternary complex containing CDC20<sup>[21,22]</sup>. DTL, BLM, BRCA1, and E2F5 are also known regulators of the G<sub>2</sub>/M checkpoint<sup>[23-26]</sup>. One possible mechanism by which NKCC1 changes the expression of these major G<sub>2</sub>/M checkpoint-related genes may be through the regulation of intracellular Cl<sup>-</sup> concentrations ([Cl]<sub>i</sub>). Recent reports have indicated that [Cl]<sub>i</sub> is a fundamental signal mediator for the regulation of various cellular functions<sup>[27-29]</sup>. For example, our study showed that [Cl]<sub>i</sub> could act as a signal to regulate mRNA expression of the epithelial Na<sup>+</sup> channel *via* a protein tyrosine kinase-dependent pathway in renal epithelial cells<sup>[29]</sup>. We have also previously shown that [Cl]<sub>i</sub> regulated cell proliferation in gastric and prostate cancer cells<sup>[5-9]</sup>. We consider NKCC to be one of the important transporters that regulates [Cl]<sub>i</sub> in the steady state and have previously shown that the blockage of NKCC decreased [Cl]<sub>i</sub><sup>[9]</sup>. Although the detailed mechanism should be verified by further studies, these observations suggest that the change in [Cl]<sub>i</sub> induced by NKCC1 may be a critically important messenger that regulates the expression of these G<sub>2</sub>/M checkpoint-related genes in ESCC cells.

Our results demonstrate that no correlation was found between NKCC1 expression and the Ki-67 labeling index in immunohistochemical studies of ESCC expres-

sion. Ki-67 is commonly used to assess cell proliferation, and this factor reacts with a nuclear antigen present throughout the cell cycle (late G<sub>1</sub>, S, G<sub>2</sub>, and M phase) of proliferating cells but is absent from quiescent (G<sub>0</sub>) cells<sup>[30]</sup>. In the present study, we found that NKCC1 plays an important role in the G<sub>2</sub>/M phase of the cell cycle. The different rates of progression through each phase of the cell cycle may explain why no correlation was found between NKCC1 and Ki-67 expression, although further studies will be needed with a larger sample size to confirm these observations. Furthermore, in the present study NKCC1 expression was correlated with the degree of histological differentiation in SCC. Similarly, we previously found that mRNA levels and the functional expression levels of NKCC1 were higher in poorly differentiated type gastric adenocarcinoma cells compared to differentiated cells<sup>[8]</sup>. Furosemide (a NKCC blocker and a loop diuretic) is often used as a diuretic to maintain urine output and improve edema, ascites, or pleural effusion for the treatment of patients with terminal stage cancers. From this viewpoint, our observation that the blockage of NKCC1 diminished the proliferation of ESCC cells provides strong clinical evidence that furosemide can be used for ESCC patients with high NKCC1 expression, such as those with poorly differentiated SCC, and suggests the possibility of a novel tailor-made treatment.

In summary, we found that NKCC1 plays a role in the proliferation of ESCC cells. An immunohistochemical analysis revealed that the expression of NKCC1 in human ESCC samples was related to the histological type of ESCC. Our microarray results also suggest that NKCC1 exhibits marked effects on the expression of genes related to G<sub>2</sub>/M cell cycle progression. A deeper understanding of the role of NKCC1 may lead to its use as an important biomarker of tumor development and/or a novel therapeutic target for ESCC.

## COMMENTS

### Background

The roles of ion transporters have recently been studied in cancer cells, and several reports have demonstrated the important roles of Cl<sup>-</sup> channels/transporters in gastrointestinal cancer cells.

### Research frontiers

Although previous reports showed that the Na<sup>+</sup>/K<sup>+</sup>/2Cl<sup>-</sup> cotransporter 1 (NKCC1) plays an important role in the proliferation of several types of cancer cells, its role in esophageal squamous cell carcinoma (ESCC) cells has not been fully investigated. Furthermore, the clinicopathological meaning of NKCC1 expression in ESCCs remains uncertain.

### Innovations and breakthroughs

The authors analyzed the expression of NKCC1 in human ESCC samples and determined its relationship with the degree of histological differentiation of SCC samples. Depletion of NKCC1 in KYSE170 cells inhibited cell proliferation *via* G<sub>2</sub>/M phase arrest. The results of microarray showed that the top-ranked canonical pathway was the G<sub>2</sub>/M DNA damage checkpoint regulation pathway, which involves MAD2L1, DTL, BLM, CDC20, BRCA1, and E2F5.

### Applications

The study results suggest that a deeper understanding of the role of NKCC1 may lead to its use as an important biomarker of tumor development and/or a novel therapeutic target for ESCC. The observation that the blockage of

NKCC1 diminished the proliferation of ESCC cells provides clinical evidence that furosemide can be used for ESCC patients with high NKCC1 expression, and suggests the possibility of a novel tailor-made treatment.

### Terminology

NKCC is a member of the cation-chloride cotransporter family. NKCC transports one sodium ion, one potassium ion, and two chloride ions across the plasma membrane and is sensitive to loop diuretics. There are two isoforms of NKCC, and NKCC1 is ubiquitously expressed in various types of cells including epithelial cells.

### Peer review

This is a good descriptive study in which the authors analyzed the role of NKCC1 in the proliferation of ESCC. The authors showed NKCC1 was found in the cytoplasm and related to tumor differentiation in patients with ESCC. Depletion of NKCC1 lead to inhibition of cell proliferation, and microarray analysis showed that NKCC1 exhibits marked effects on the expression of genes related to G<sub>2</sub>/M cell cycle progression. The results are interesting and meaningful for further understand the role of NKCC1 on cancer development.

## REFERENCES

- Bustin SA, Li SR, Dorudi S. Expression of the Ca<sup>2+</sup>-activated chloride channel genes CLCA1 and CLCA2 is down-regulated in human colorectal cancer. *DNA Cell Biol* 2001; 20: 331-338 [PMID: 11445004 DOI: 10.1089/10445490152122442]
- Sarosi GA, Jaiswal K, Herndon E, Lopez-Guzman C, Spechler SJ, Souza RF. Acid increases MAPK-mediated proliferation in Barrett's esophageal adenocarcinoma cells via intracellular acidification through a Cl<sup>-</sup>/HCO<sub>3</sub><sup>-</sup> exchanger. *Am J Physiol Gastrointest Liver Physiol* 2005; 289: G991-G997 [PMID: 16081761 DOI: 10.1152/ajpgi.00215.2005]
- Hebert SC, Mount DB, Gamba G. Molecular physiology of cation-coupled Cl<sup>-</sup> cotransport: the SLC12 family. *Pflugers Arch* 2004; 447: 580-593 [PMID: 12739168 DOI: 10.1007/s00424-003-1066-3]
- Mount DB, Mercado A, Song L, Xu J, George AL, Delpire E, Gamba G. Cloning and characterization of KCC3 and KCC4, new members of the cation-chloride cotransporter gene family. *J Biol Chem* 1999; 274: 16355-16362 [PMID: 10347194 DOI: 10.1152/physrev.00011.2004]
- Shiozaki A, Otsuji E, Marunaka Y. Intracellular chloride regulates the G<sub>1</sub>/S cell cycle progression in gastric cancer cells. *World J Gastrointest Oncol* 2011; 3: 119-122 [PMID: 22007274 DOI: 10.4251/wjgo.v3.i8.119]
- Miyazaki H, Shiozaki A, Niisato N, Ohsawa R, Itoi H, Ueda Y, Otsuji E, Yamagishi H, Iwasaki Y, Nakano T, Nakahari T, Marunaka Y. Chloride ions control the G<sub>1</sub>/S cell-cycle checkpoint by regulating the expression of p21 through a p53-independent pathway in human gastric cancer cells. *Biochem Biophys Res Commun* 2008; 366: 506-512 [PMID: 18067855 DOI: 10.1016/j.bbrc.2007.11.144]
- Ohsawa R, Miyazaki H, Niisato N, Shiozaki A, Iwasaki Y, Otsuji E, Marunaka Y. Intracellular chloride regulates cell proliferation through the activation of stress-activated protein kinases in MKN28 human gastric cancer cells. *J Cell Physiol* 2010; 223: 764-770 [PMID: 20205250 DOI: 10.1002/jcp.22088]
- Shiozaki A, Miyazaki H, Niisato N, Nakahari T, Iwasaki Y, Itoi H, Ueda Y, Yamagishi H, Marunaka Y. Furosemide, a blocker of Na<sup>+</sup>/K<sup>+</sup>/2Cl<sup>-</sup> cotransporter, diminishes proliferation of poorly differentiated human gastric cancer cells by affecting G<sub>0</sub>/G<sub>1</sub> state. *J Physiol Sci* 2006; 56: 401-406 [PMID: 17052386 DOI: 10.2170/physiolsci.RP010806]
- Hiraoka K, Miyazaki H, Niisato N, Iwasaki Y, Kawachi A, Miki T, Marunaka Y. Chloride ion modulates cell proliferation of human androgen-independent prostatic cancer cell. *Cell Physiol Biochem* 2010; 25: 379-388 [PMID: 20332618 DOI: 10.1159/000303042]
- Nishihira T, Hashimoto Y, Katayama M, Mori S, Kuroki T. Molecular and cellular features of esophageal cancer cells. *J Cancer Res Clin Oncol* 1993; 119: 441-449 [PMID: 8509434]
- Shimada Y, Imamura M, Wagata T, Yamaguchi N, Tobe T. Characterization of 21 newly established esophageal cancer cell lines. *Cancer* 1992; 69: 277-284 [PMID: 1728357]
- Sobin L, Gospodarowicz M, Wittekind C, eds. TNM Classification of malignant tumors. 7th ed. Hoboken, NJ: John Wiley Sons, Inc, 2009
- Remmele W, Stegner HE. [Recommendation for uniform definition of an immunoreactive score (IRS) for immunohistochemical estrogen receptor detection (ER-ICA) in breast cancer tissue]. *Pathologe* 1987; 8: 138-140 [PMID: 3303008]
- Kunzelmann K. Ion channels and cancer. *J Membr Biol* 2005; 205: 159-173 [PMID: 16362504 DOI: 10.1007/s00232-005-0781-4]
- Schönherr R. Clinical relevance of ion channels for diagnosis and therapy of cancer. *J Membr Biol* 2005; 205: 175-184 [PMID: 16362505 DOI: 10.1007/s00232-005-0782-3]
- Lastraioli E, Guasti L, Crociari O, Polvani S, Hofmann G, Witchel H, Bencini L, Calistri M, Messerini L, Scatizzi M, Moretti R, Wanke E, Olivotto M, Mugnai G, Arcangeli A. hERG1 gene and HERG1 protein are overexpressed in colorectal cancers and regulate cell invasion of tumor cells. *Cancer Res* 2004; 64: 606-611 [PMID: 14744775 DOI: 10.1158/0008-5472.CAN-03-2360]
- Kim CJ, Cho YG, Jeong SW, Kim YS, Kim SY, Nam SW, Lee SH, Yoo NJ, Lee JY, Park WS. Altered expression of KCNK9 in colorectal cancers. *APMIS* 2004; 112: 588-594 [PMID: 15601307 DOI: 10.1111/j.1600-0463.2004.apm1120905.x]
- Shao XD, Wu KC, Hao ZM, Hong L, Zhang J, Fan DM. The potent inhibitory effects of cisapride, a specific blocker for human ether-a-go-go-related gene (HERG) channel, on gastric cancer cells. *Cancer Biol Ther* 2005; 4: 295-301 [PMID: 15846098 DOI: 10.4161/cbt.4.3.1500]
- Wang XT, Nagaba Y, Cross HS, Wrba F, Zhang L, Guggino SE. The mRNA of L-type calcium channel elevated in colon cancer: protein distribution in normal and cancerous colon. *Am J Pathol* 2000; 157: 1549-1562 [PMID: 11073814 DOI: 10.1016/S0002-9440(10)64792-X]
- Tsavaler L, Shapero MH, Morkowski S, Laus R. Trp-p8, a novel prostate-specific gene, is up-regulated in prostate cancer and other malignancies and shares high homology with transient receptor potential calcium channel proteins. *Cancer Res* 2001; 61: 3760-3769 [PMID: 11325849]
- Luo X, Fang G, Coldiron M, Lin Y, Yu H, Kirschner MW, Wagner G. Structure of the Mad2 spindle assembly checkpoint protein and its interaction with Cdc20. *Nat Struct Biol* 2000; 7: 224-229 [PMID: 10700282 DOI: 10.1038/73338]
- Luo X, Tang Z, Xia G, Wassmann K, Matsumoto T, Rizo J, Yu H. The Mad2 spindle checkpoint protein has two distinct natively folded states. *Nat Struct Mol Biol* 2004; 11: 338-345 [PMID: 15024386 DOI: 10.1016/S1097-2765(01)00435-X]
- Sansam CL, Shepard JL, Lai K, Ianari A, Danielian PS, Amsterdam A, Hopkins N, Lees JA. DTL/CDT2 is essential for both CDT1 regulation and the early G<sub>2</sub>/M checkpoint. *Genes Dev* 2006; 20: 3117-3129 [PMID: 17085480 DOI: 10.1101/gad.1482106]
- Ababout M, Dutertre S, Lécluse Y, Onclercq R, Chatton B, Amor-Guérét M. ATM-dependent phosphorylation and accumulation of endogenous BLM protein in response to ionizing radiation. *Oncogene* 2000; 19: 5955-5963 [PMID: 11146546]
- Shabbeer S, Omer D, Berneman D, Weitzman O, Alpaugh A, Pietraszkiewicz A, Metsuyanum S, Shainskaya A, Papa MZ, Yarden RI. BRCA1 targets G<sub>2</sub>/M cell cycle proteins for ubiquitination and proteasomal degradation. *Oncogene* 2013; 32: 5005-5016 [PMID: 23246971 DOI: 10.1038/onc.2012.522]
- Wan Z, Zhi N, Wong S, Keyvanfar K, Liu D, Raghavachari N, Munson PJ, Su S, Malide D, Kajigaya S, Young NS. Human parvovirus B19 causes cell cycle arrest of human erythroid progenitors via deregulation of the E2F family of transcription factors. *J Clin Invest* 2010; 120: 3530-3544 [PMID:

- 20890043 DOI: 10.1172/JCI41805]
- 27 Jiang B, Hattori N, Liu B, Nakayama Y, Kitagawa K, Sumita K, Inagaki C. Expression and roles of Cl<sup>-</sup> channel ClC-5 in cell cycles of myeloid cells. *Biochem Biophys Res Commun* 2004; 317: 192-197 [PMID: 15047167 DOI: 10.1016/j.bbrc.2004.03.036]
- 28 Menegazzi R, Busetto S, Dri P, Cramer R, Patriarca P. Chloride ion efflux regulates adherence, spreading, and respiratory burst of neutrophils stimulated by tumor necrosis factor-alpha (TNF) on biologic surfaces. *J Cell Biol* 1996; 135: 511-522 [PMID: 8896606]
- 29 Niisato N, Eaton DC, Marunaka Y. Involvement of cytosolic Cl<sup>-</sup> in osmoregulation of alpha-ENaC gene expression. *Am J Physiol Renal Physiol* 2004; 287: F932-F939 [PMID: 15292045 DOI: 10.1152/ajprenal.00131.2004]
- 30 Gerdes J, Lemke H, Baisch H, Wacker HH, Schwab U, Stein H. Cell cycle analysis of a cell proliferation-associated human nuclear antigen defined by the monoclonal antibody Ki-67. *J Immunol* 1984; 133: 1710-1715 [PMID: 6206131]

P- Reviewers: Kim MP, Zhao BS  
S- Editor: Qi Y L- Editor: A E- Editor: Liu XM







Published by Baishideng Publishing Group Inc  
8226 Regency Drive, Pleasanton, CA 94588, USA  
Telephone: +1-925-223-8242  
Fax: +1-925-223-8243  
E-mail: [bpgoffice@wjgnet.com](mailto:bpgoffice@wjgnet.com)  
Help Desk: <http://www.wjgnet.com/esps/helpdesk.aspx>  
<http://www.wjgnet.com>



ISSN 1007-9327



© 2014 Baishideng Publishing Group Inc. All rights reserved

## Perioperative outcomes of esophagectomy preceded by the laparoscopic transhiatal approach for esophageal cancer

A. Shiozaki, H. Fujiwara, Y. Murayama, S. Komatsu, Y. Kuriu, H. Ikoma, M. Nakanishi, D. Ichikawa, K. Okamoto, T. Ochiai, Y. Kokuba, E. Otsuji

*Division of Digestive Surgery, Department of Surgery, Kyoto Prefectural University of Medicine, Kyoto, Japan*

**SUMMARY.** This study was designed to determine the efficacy of esophagectomy preceded by the laparoscopic transhiatal approach (LTHA) with regard to the perioperative outcomes of esophageal cancer. The esophageal hiatus was opened by hand-assisted laparoscopic surgery, and carbon dioxide was introduced into the mediastinum. Dissection of the distal esophagus was performed up to the level of the tracheal bifurcation. En bloc dissection of the posterior mediastinal lymph nodes was performed using LTHA. Next, cervical lymphadenectomy, reconstruction via a retrosternal route with a gastric tube and anastomosis from a cervical approach were performed. Finally, a small thoracotomy (around 10 cm in size) was made to extract the thoracic esophagus and allow upper mediastinal lymphadenectomy to be performed. The treatment outcomes of 27 esophageal cancer patients who underwent LTHA-preceding esophagectomy were compared with those of 33 patients who underwent the transthoracic approach preceding esophagectomy without LTHA (thoracotomy; around 20 cm in size). The intrathoracic operative time and operative bleeding were significantly decreased by LTHA. The total operative time did not differ between the two groups, suggesting that the abdominal procedure was longer in the LTHA group. The number of resected lymph nodes did not differ between the two groups. Postoperative respiratory complications occurred in 18.5% of patients treated with LTHA and 30.3% of those treated without it. The increase in the number of peripheral white blood cells and the duration of thoracic drainage were significantly decreased by this method. Our surgical procedure provides a good surgical view of the posterior mediastinum, markedly shortens the intrathoracic operative time, and decreases the operative bleeding without increasing major postoperative complications.

**KEY WORDS:** esophageal cancer, laparoscopic transhiatal approach, perioperative outcome.

### INTRODUCTION

The surgical trauma caused by thoracoabdominal esophagectomy is perhaps greater than that caused by all other general surgical operations.<sup>1–3</sup> Recent reports have shown that using thoracoscopic esophagectomy minimizes the injury to the chest wall and reduces surgical invasiveness.<sup>4–8</sup> Although the efficacy of these procedures has been actively discussed, several problems remain, for instance, difficulties in maintaining the surgical field, the necessity of mastering the required skills, and the long intrathoracic operative time.

From 2007, we started performing hand-assisted laparoscopic surgery (HALS) for esophagectomy

combined with gastric tube reconstruction. On the other hand, intrathoracic operations are performed via a small right thoracotomy under the assistance of thoracoscopy in the left lateral-decubitus position. However, it is difficult to maintain the surgical field in the lower mediastinum using this transthoracic approach. In this context, by applying the HALS technique to mediastinal operations, we recently started to perform esophagectomy preceded by the laparoscopic transhiatal approach (LTHA) for patients with esophageal cancer.<sup>9,10</sup> In this method, carbon dioxide is introduced into the mediastinum from the abdominal side; and middle and lower mediastinal operations can be performed via a transhiatal approach. The main advantages of this method are that a good surgical view of the posterior and left mediastinum is obtained and that the quality of mediastinal lymph node dissection can be improved. In addition, by performing the reconstruction prior to

Address correspondence to: Dr Hitoshi Fujiwara, MD, PhD, Division of Digestive Surgery, Department of Surgery, Kyoto Prefectural University of Medicine, 465 Kajii-cho, Kamigyo-ku, Kyoto 602-8566, Japan. Email: hfuji@koto.kpu-m.ac.jp

esophagectomy, the thoracic procedures performed via the right thoracotomy can be simplified, and the intrathoracic operative time can be shortened.

Here, we describe the surgical technique of our method in detail and analyze the perioperative treatment outcomes of patients treated with LTHA to determine the efficacy of this method. Our results revealed that our method markedly shortened the intrathoracic operative time; decreased intraoperative bleeding, and postoperative thoracic discharge without increasing major complications.

## PATIENTS AND METHODS

### Surgical procedure

A mediastinal operation, which was performed from the abdominal side, and a cervical operation were performed before thoracotomy; thus, the patients were placed in a supine position on the operating table with both arms tucked by their sides. At first, an abdominal operation was performed using HALS, and subsequently, middle and lower mediastinal operations were performed using LTHA. An upper abdominal incision (70 mm) was made, and a Lap Disc (regular) (Ethicon, Cincinnati, OH) was put in place (Fig. 1). Three 12 mm ports were produced, one in each flank and one in the left hypochondrium, and one 5 mm port for the flexible laparoscope was inserted into the lower abdomen (Fig. 1). The operator stood on the right side of the patient and inserted the Lap Disc with their left hand, and the 12 mm port in the right flank was mainly used for surgery. The assistant stood on the left side of patient, and the ports in the left abdomen were used to provide assistance. The scopist stood near the patient's crotch. Carbon dioxide was introduced into the intra-

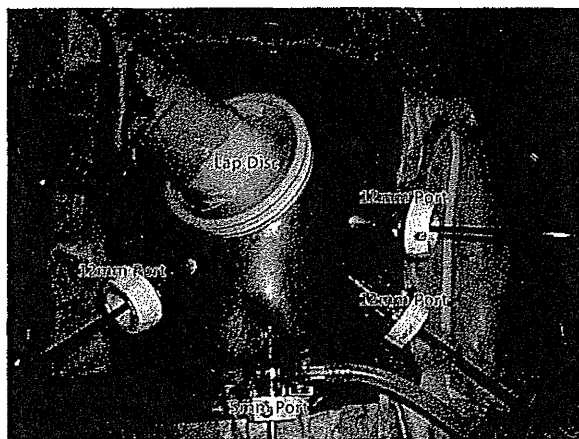


Fig. 1 Intraoperative view of the trocars and incision locations on the abdomen. A Lap Disc (regular) was placed in the upper abdomen. Three 12 mm ports were inserted, one in each flank and one in the left hypochondrium, and one 5 mm port for the videoscope was inserted in the lower abdomen.

© 2012 Copyright the Authors

Journal compilation © 2012, Wiley Periodicals, Inc. and the International Society for Diseases of the Esophagus

abdominal space, and the pneumoperitoneum pressure was controlled at 10 mmHg.<sup>10</sup>

At first, the operator lifted up the stomach with their left hand, and then the greater omentum, the left gastroepiploic vessels, and the gastrosplenic ligament were divided using the EnSeal device (Ethicon, Somerville, NJ, USA) (Fig. 2A). After that, the esophageal hiatus was opened, and carbon dioxide was introduced into the mediastinum (Fig. 2B). The abovementioned 5 mm flexible laparoscope was also used for the mediastinal dissection. The assistant inserted an ENDO RETRACT (Autosuture Norwalk, CT) and a blunt tip dissector through the ports on the left side; and the working space in the mediastinum was secured with these two devices and 10 mmHg of pneumomediastinum pressure. As we did not make an incision in the left mediastinal pleura, the left and posterior mediastinal spaces were inflated, and sufficient working space was obtained (Fig. 2C). Dissection of the anterior and left side of the distal esophagus up to the level of the tracheal bifurcation was performed with the EnSeal device and the blunt tip dissector. Using this approach, dissection of the anterior sides of the posterior mediastinal lymph nodes was easy to perform (Fig. 2D).<sup>10</sup>

Next, the adventitia of the thoracic aorta was exposed at the level of the crural of the diaphragm, and gentle dissection of the anterior side of the thoracic aorta to the cranial side was performed (Fig. 3A). In general, one or two roots of the proper esophageal arteries were confirmed, and we were able to divide them safely using the EnSeal device under a magnified videoscopic view (Fig. 3B). After these procedures, both the anterior and posterior sides of the posterior mediastinal lymph nodes including the thoracic paraaortic and left pulmonary ligament lymph nodes were dissected. While lifting these lymph nodes like a membrane, we cut them along the borderline of the left mediastinal pleura (Fig. 3C). In this manner, the posterior mediastinal and left main bronchus lymph nodes were dissected en bloc.<sup>10</sup>

The dissection of posterior mediastinal lymph nodes was extended toward the caudal side from the crural of the diaphragm to the celiac artery. Thus, the lymph nodes in the esophageal hiatus of the diaphragm, the infradiaphragmatic lymph nodes, and the lymph nodes along the celiac artery were dissected en bloc from the left side. After that, the left gastric vessels were clipped and divided, and the lymph nodes along the left gastric artery were dissected. Finally, dissection of the posterior and right sides of the distal esophagus was performed, and an incision was made in the right mediastinal pleura to allow dissection to be performed. The right mediastinal pleural incision was then extended to the lower margin of the arch of the azygos vein (Fig. 3D). Thus, the middle and lower thoracic esophagus was completely detached from the surrounding tissue.

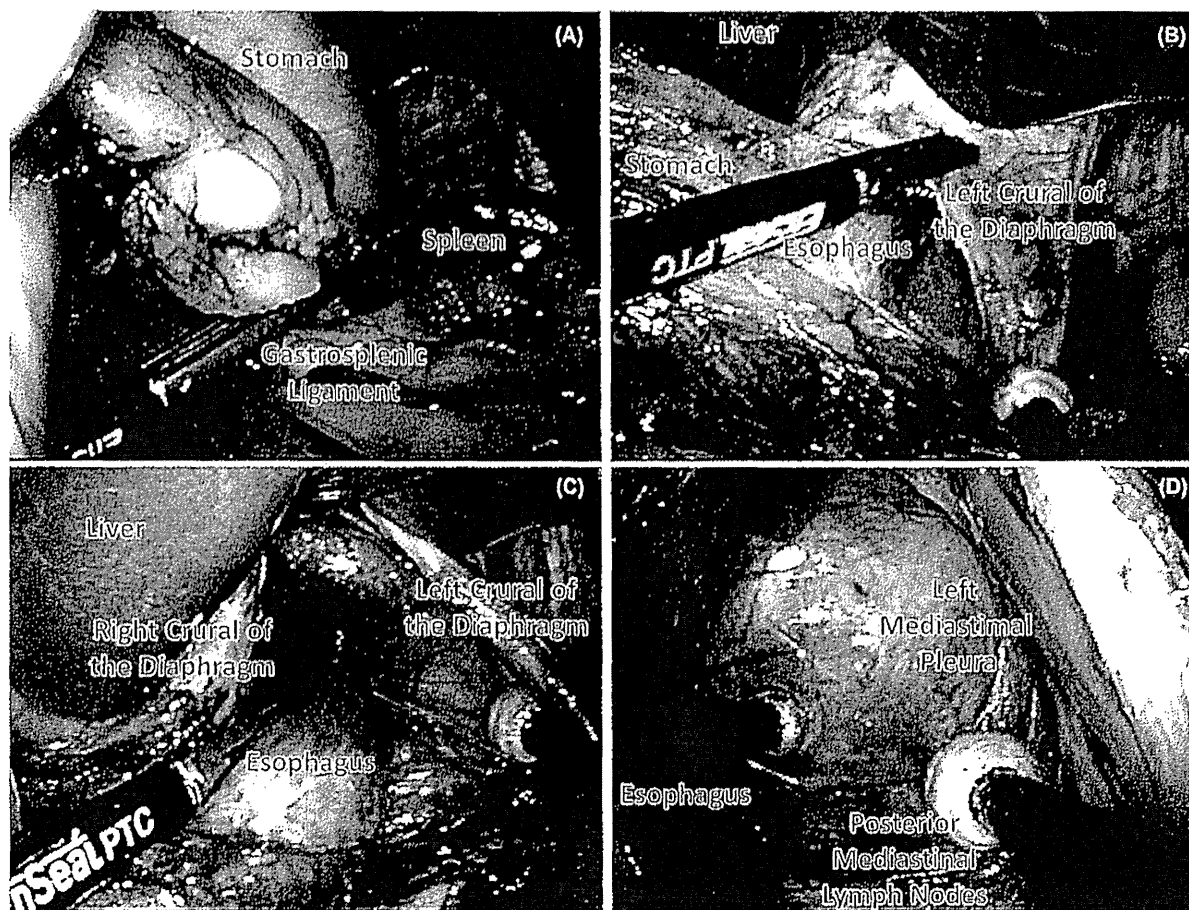


Fig. 2 (A) The operator lifted up the stomach using their left hand, and the gastrosplenic ligament was divided using the EnSeal device. (B) The esophageal hiatus was divided, and carbon dioxide was introduced into the mediastinum. (C) The working space in the mediastinum was secured an ENDO RETRACT, a blunt tip dissector, and pneumomediastinum pressure. (D) Dissection of the anterior and left side of the distal esophagus was performed with the EnSeal device up to the level of the tracheal bifurcation.

After the division of the abdominal esophagus, a collar incision was made in the neck, and cervical and upper mediastinal lymph node dissection (including the cranial half of the left recurrent nerve lymph nodes) was performed. After the cervical esophagus was divided, an abdominal spatula was inserted via an upper abdominal incision which was used for HALS to dissect retrosternal space. Then, reconstruction was performed via a retrosternal route with a gastric tube, as this method prevents recurrent intrathoracic locoregional tumor cells from invading the neo-esophagus.<sup>11,12</sup> The esophagogastric anastomosis was performed by hand from the cervical approach.

Finally, in the left lateral-decubitus position, a small right thoracotomy was made (around 10 cm in size), and rib spreader was used to maintain the small surgical field. The extraction of the thoracic esophagus and upper mediastinal lymph node dissection were performed under the assistance of thoracoscopy. Using this approach, the dissection of the caudal half of the left recurrent nerve lymph nodes

and the left tracheobronchial lymph nodes, which we could not reach from above or below, was performed. A 10 cm thoracotomy and one endoscopic port were sufficient for the thoracic procedure because we had performed the middle and lower mediastinal lymphadenectomy via the LTHA.

#### Patients

We started to routinely perform LTHA-preceding esophagectomy for patients with esophageal cancer in April 2010. From January 2009 to December 2010, a total of 60 patients with esophageal squamous cell carcinoma (SCC) underwent subtotal esophagectomy combined with extensive lymph node dissection and gastric tube reconstruction via a retrosternal route at the Division of Digestive Surgery, Department of Surgery, Kyoto Prefectural University of Medicine. These patients were retrospectively divided into two groups according to the operative method, with (27 patients; April 2010–December 2010) or without (33 patients; January 2009–March 2010) LTHA, and

© 2012 Copyright the Authors

Journal compilation © 2012, Wiley Periodicals, Inc. and the International Society for Diseases of the Esophagus

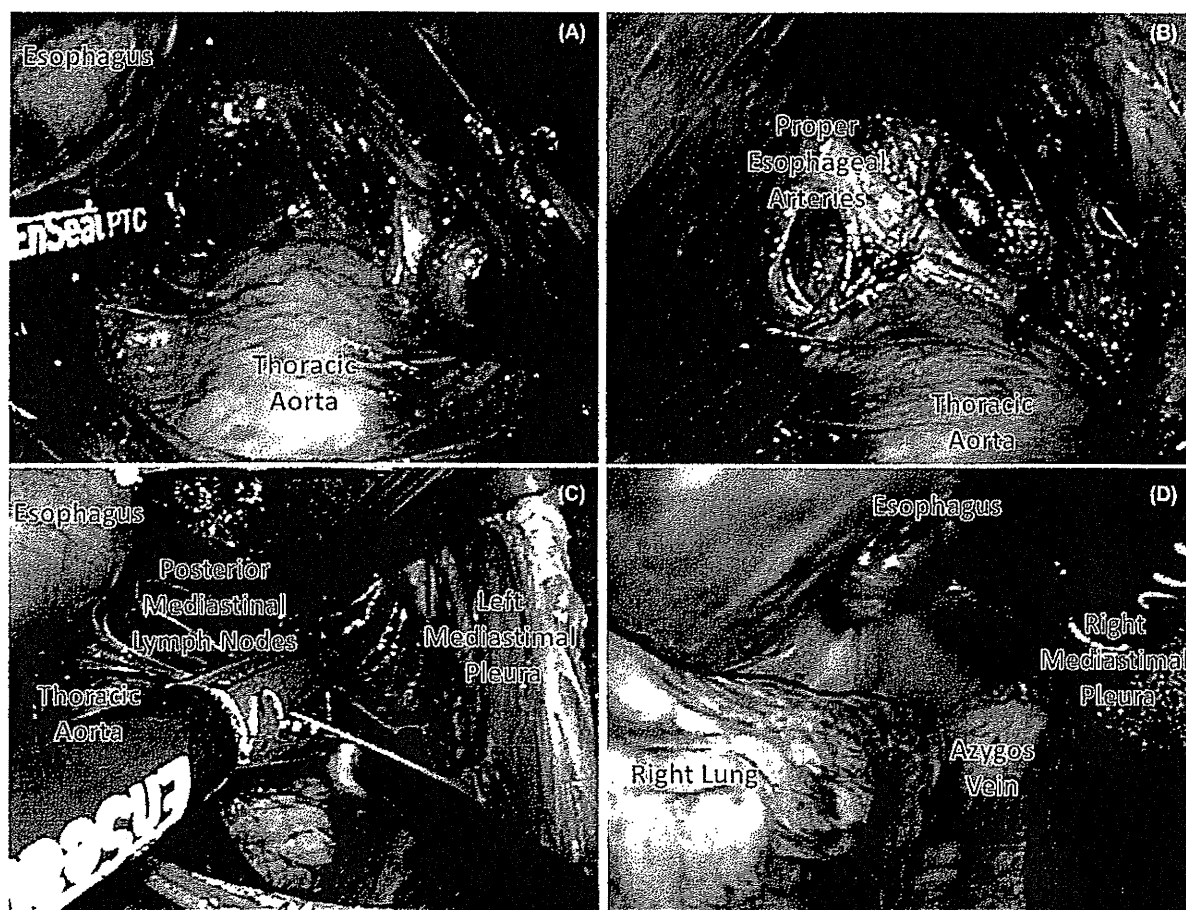


**Fig. 3** (A) The adventitia of the thoracic aorta was exposed near to the crural of the diaphragm, and dissection of the anterior side of the thoracic aorta was performed. (B) The roots of the proper esophageal arteries were confirmed under a magnified videoscopic view. (C) En bloc dissection of the posterior mediastinal lymph nodes (thoracic paraaortic and left pulmonary ligament lymph nodes). Both the anterior and posterior sides of the posterior mediastinal lymph nodes were resected. While lifting up these lymph nodes like a membrane, they were cut along the borderline of the left mediastinal pleura. (D) An incision was made in the right mediastinal pleura and was extended to the inferior margin of the arch of the azygos vein.

these two groups were compared with respect to the perioperative treatment outcome. For both groups, the operative indication was completely same, namely operations were performed in patients with clinical T1-3, N0-3, M0 esophageal cancer based on 7th TNM staging systems (UICC International Union Against Cancer TNM Classification of Malignant Tumours; 7th Edition).<sup>13</sup> All patients were treated by two highly skilled surgeons; and informed consent was obtained from each participant.

For 33 patients who underwent subtotal esophagectomy without LTHA, thoracic surgery was performed first (thoracotomy; around 20 cm in size) under the assistance of thoracoscopy, and then abdominal surgery was performed using HALS. Finally, cervical lymph node dissection, reconstruction via a retrosternal route with a gastric tube, and anastomosis from a cervical approach were performed. The sizes of the cervical and abdominal incisions and the locations of the trocars used in these 33

patients were almost the same as those employed for the LTHA-treated patients.

A total of 22 patients (with LTHA: 12 patients/without LTHA: 10 patients) underwent three-field lymphadenectomy, and a total of 38 patients (with LTHA: 15 patients/without LTHA: 23 patients) underwent two-field lymphadenectomy. A total of 42 patients (with LTHA: 22 patients/without LTHA: 20 patients) received preoperative chemotherapy involving two courses of cisplatin (80 mg/m<sup>2</sup>/day, day1) plus 5-fluorouracil (800 mg/m<sup>2</sup>/day, day1-5).<sup>14</sup>

To compare the backgrounds of these two groups, we analyzed their clinicopathological features, such as age, gender, primary tumor location, histological type of SCC, TNM category, and pathological stage. Histopathological examinations were performed on the primary lesions and all dissected lymph nodes using serial sections. All histopathological diagnoses were performed by experienced pathologists. The TNM category and pathological stage were classified

according to the pTNM Pathological Classification.<sup>13</sup> The effects of preoperative comorbidities were analyzed using the Charlson comorbidity index.<sup>15</sup>

To determine the efficacy of LTHA, the two groups were compared with respect to several perioperative factors, such as the total operative time, intrathoracic operative time, operative bleeding, number of resected lymph nodes, extubation time, frequency of postoperative respiratory complications, number of white blood cells, serum C-reactive protein (CRP), and the duration of thoracic drainage, frequency of recurrent nerve palsy and anastomotic leakage. The number of peripheral white blood cells and the serum CRP level were measured at 2 and 7 days after the operation. According to our criteria, the thoracic drainage tube was removed when the amount of thoracic discharge fell below 150 mL/day. Postoperative respiratory complications were defined as those involving major respiratory insufficiency; i.e. a need for reintubation or severe pneumonia. Recurrent nerve palsy was diagnosed by otolaryngologists using a laryngoscope when the extubation was performed.

Statistical analysis was carried out using the Student's *t*-test and Fisher's exact test. Differences were considered significant when the *P*-value was less than 0.05. All analyses were performed using statistical software (JMP, version 5; SAS Institute Inc., Cary, NC).

## RESULTS

Sixty patients with esophageal cancer who underwent subtotal esophagectomy combined with gastric tube reconstruction via a retrosternal route were divided into two groups according to the operative procedure they underwent; i.e. with (27 patients) and without LTHA (33 patients) groups. There were no significant differences between the background clinicopathological parameters of the two groups (such as age, gender, primary tumor location, histological type of SCC, TNM category, pathological stage, Charlson comorbidity index, or the number of lymphadenectomy fields) (Table 1). One patient treated without LTHA was pathologically diagnosed as pT4 (aorta). A total five patients (with LTHA: three patients/without LTHA: two patients) were pathologically diagnosed as pM1 because of supraclavicular lymph nodes metastases.

We performed the comparison of intraoperative factors between two groups. The total operative time did not differ between the two groups (with LTHA: 408.7 ± 11.2 min/without LTHA: 414.3 ± 10.1 min) (mean ± SEM) (Fig. 4A). The intrathoracic operative time was significantly shorter in the patients treated with LTHA (60.8 ± 3.5 min) than in the patients treated without LTHA (138.3 ± 3.2 min) (Fig. 4B).

**Table 1** Comparison of the background clinicopathological parameters of the patients treated with and without laparoscopic transhiatal approach (LTHA) prior to thoracotomy

Variables	LTHA		<i>P</i> -value
	(+)	(-)	
Age			
65 years or more	13	21	0.298
Less than 65 years	14	12	
Gender			
Male	21	30	0.276
Female	6	3	
Location of Primary Tumor			
Ce-Ut	6	7	1.000
Mt-Lt	21	26	
Histological type of SCC			
Well-moderately differentiated	20	22	0.582
Poorly differentiated	7	11	
pT Category			
pT1-2	17	19	0.793
pT3-4	10	14	
pN Category			
pN0	10	17	0.305
pN1-3	17	16	
pM Category			
pM0	24	31	0.649
pM1	3	2	
Pathological Stage			
pStage 0-II	15	18	1.000
pStage III-IV	12	15	
Charlson Comorbidity Index			
≥2	24	29	1.000
<2	3	4	
No. of Lymphadenectomy Fields			
Two	15	23	0.292
Three	12	10	

Ce, cervical esophagus; Lt, lower thoracic esophagus; Mt, middle thoracic esophagus; Ut, upper thoracic esophagus.

Total operative bleeding was significantly reduced in the patients treated with LTHA (302.6 ± 44.4 mL) in comparison with the patients treated without LTHA (426.3 ± 40.7 mL) (Fig. 4C). Furthermore, the total number of resected lymph nodes did not differ between the two groups (with LTHA: 47.2 ± 5.0 /without LTHA: 43.7 ± 4.5) (Fig. 4D). The total number of resected thoracic lymph nodes did not differ between the two groups (with LTHA: 17.7 ± 8.3, without LTHA: 21.3 ± 1.5; *P* = 0.122). These results suggest that LTHA-preceding esophagectomy can be used to reduce the intrathoracic operative time and the total operative bleeding without diminishing the quality of lymph node dissection.

Next, we performed the comparison of postoperative factors between the two groups (Table 2). The extubation time after surgery did not differ between the two groups. Postoperative respiratory complications occurred in 18.5% of the patients treated with LTHA (pneumonia: five patients), whereas they occurred in 30.3% of the patients treated without LTHA (pneumonia: eight patients, ARDS: 2 patients) without significant difference. We analyzed the number of peripheral white blood cells and the serum CRP level at 2 and 7 days after the operation.

© 2012 Copyright the Authors

Journal compilation © 2012, Wiley Periodicals, Inc. and the International Society for Diseases of the Esophagus

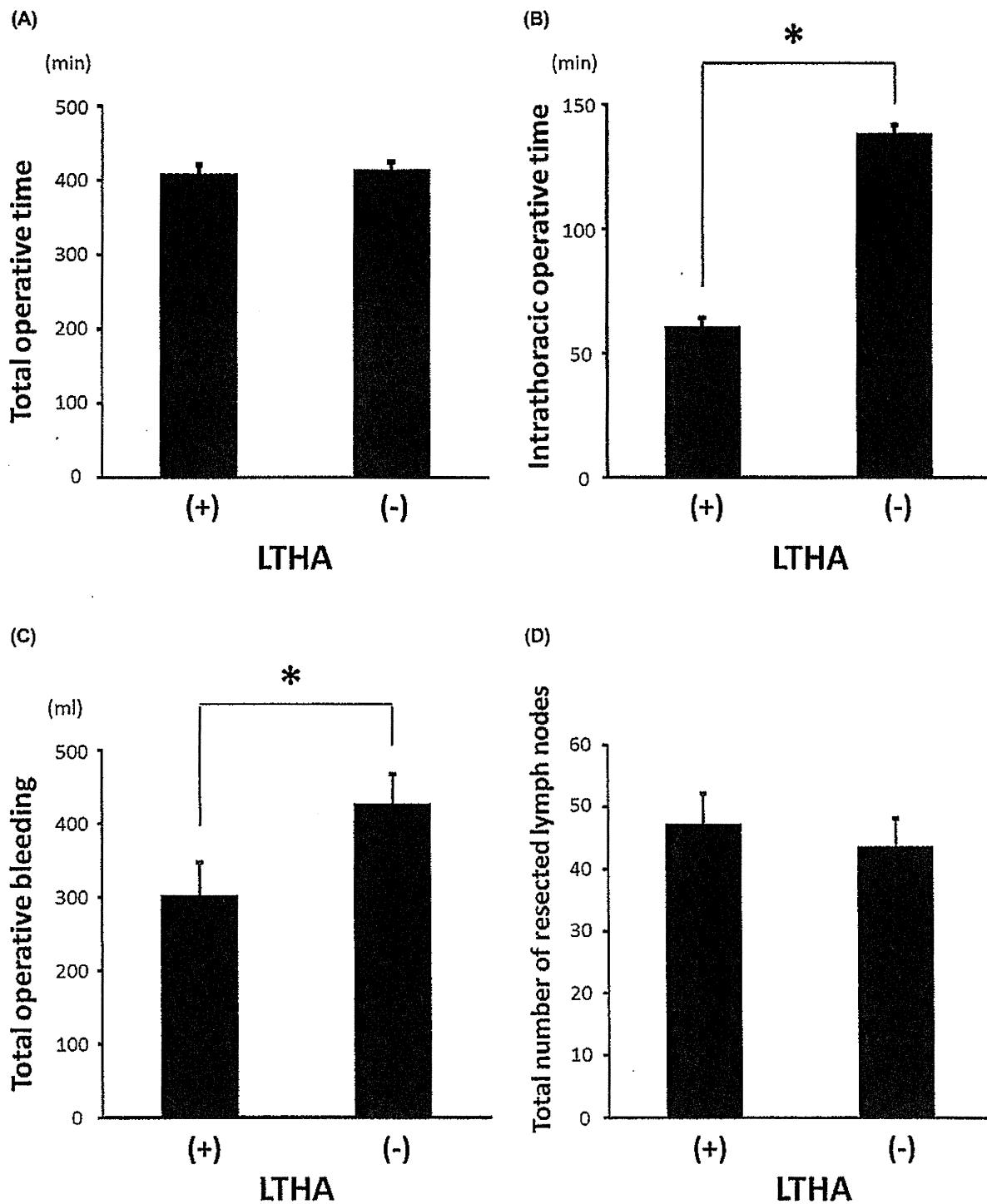


Fig. 4 Comparisons of intraoperative factors between the patients treated with and without laparoscopic transhiatal approach (LTHA) prior to thorcotomy. (A) Total operative time. (B) Intrathoracic operative time. (C) Total operative bleeding. (D) Total number of resected lymph nodes. Mean  $\pm$  SEM. \* $P < 0.05$  was considered significant.

The elevation in the number of peripheral white blood cells at 2 days after the operation was significantly inhibited in the patients treated with LTHA ( $8459 \pm 721/\mu\text{l}$ ) in comparison with those treated without LTHA ( $10\,439 \pm 652/\mu\text{l}$ ). The duration of thoracic drainage was significantly shortened in the

patients treated with LTHA ( $5.7 \pm 0.6$  days) in comparison with the patients treated without LTHA ( $9.0 \pm 0.5$  days), suggesting that this method decreased the amount of postoperative thoracic discharge by preventing damage to thoracic and mediastinal tissues. The frequency of recurrent nerve palsy and

**Table 2** Comparison of postoperative factors between the patients treated with and without laparoscopic transhiatal approach (LTHA) prior to thoracotomy

Variables	LTHA		P-value
	(+)	(-)	
Extubation time after surgery (days)	1.7 ± 0.5	1.5 ± 0.4	0.766
Postoperative respiratory complications	5/27 (18.5%)	10/33 (30.3%)	0.375
White blood cells at 2 days after surgery (/μl)	8 459 ± 721	10 439 ± 652	0.046*
at 7 days after surgery (/μl)	8 138 ± 530	8 703 ± 471	0.429
Serum CRP at 2 days after surgery (mg/dl)	20.9 ± 1.1	19.2 ± 1.0	0.254
at 7 days after surgery (mg/dl)	7.5 ± 1.1	7.6 ± 1.0	0.954
Duration of thoracic drainage (days)	5.7 ± 0.6	9.0 ± 0.5	<0.001*
Recurrent nerve palsy	11/27 (40.7%)	13/33 (39.4%)	1.000
Anastomotic leakage	1/27 (3.7%)	4/33 (12.1%)	0.367
Postoperative hospital stay (days)	44.0 ± 5.2	44.2 ± 4.7	0.976

Mean ± SEM. \*P <0.05 was considered significant. CRP, C-reactive protein.

anastomotic leakage did not differ between the two groups. These results suggest that LTHA-preceding esophagectomy could be used to improve postoperative care without increasing the risk of major complications.

## DISCUSSION

Thoracoscopic esophagectomy was reported to minimize injuries to the chest wall and reduce surgical invasiveness.<sup>4-8</sup> Although thoracoscopic esophagectomy in the left lateral-decubitus position<sup>4-6</sup> and thoracoscopic esophagectomy in the prone position<sup>7,8</sup> are widely applied methods, both require the mastery of certain skills. In thoracoscopic esophagectomy in the left lateral-decubitus position, it is difficult to maintain the surgical field in the lower mediastinum. Although we have some experience with this thoracoscopic approach, we are keenly aware of the importance of having a highly skilled assistant and scopist. In thoracoscopic esophagectomy performed with the patient in the prone position, although it is easier to maintain the surgical field in the middle and lower mediastinum in comparison with operations performed in the left lateral-decubitus position, it takes time to perform intrathoracic surgery. To perform middle and lower mediastinal operations safely and achieve satisfactory operability, we developed the LTHA-preceding esophagectomy method for patients with esophageal cancer. Since DePaula *et al.* described their transhiatal laparoscopic esophagectomy method, there have been several reports about this technique.<sup>16-18</sup> Upper mediastinal lymphadenectomy is extremely important for patients with thoracic esophageal cancer. We performed middle and lower mediastinal lymphadenectomy via the LTHA and upper mediastinal lymphadenectomy via the thoracic approach. This combined approach enabled us to increase the quality of lymphadenectomy and decrease the intrathoracic operative time.

As the duration of one-lung ventilation is known to affect postoperative immune reactions and respiratory complications, it is important to decrease the intrathoracic operative time.<sup>19,20</sup> We were able to perform middle and lower thoracic mediastinal surgery from the abdominal side using LTHA, and as we performed the reconstruction via a retrosternal route with a gastric tube prior to esophagectomy, the subsequent thoracic operations, which were performed via a right thoracotomy, concentrated on dissection of the upper mediastinum and were afforded a good surgical view and operability. Therefore, we were able to minimize the thoracic wound and decrease the intrathoracic operative time. Furthermore, we observed that the elevation in the number of peripheral white blood cells at 2 days after the operation was significantly inhibited in the patients treated with the LTHA in comparison with those treated without it, suggesting that our method inhibits excessive postoperative acute immune responses.

The main advantage of our surgical procedure is that it allows the posterior mediastinal lymph nodes including the paraaortic and left pulmonary ligament lymph nodes to be approached via the appropriate anatomical layer.<sup>10</sup> The left side of the mediastinum is a difficult space to approach via a right thoracotomy. In particular, complete resection of the left pulmonary ligament lymph nodes via a right thoracic approach carries a risk of serious complications; however, metastases and recurrent tumors sometimes develop in these lymph nodes in esophageal cancer patients. Our data showed that metastases developed in the left pulmonary ligament lymph nodes of 3.3% of esophageal squamous cell carcinoma patients (single metastasis: 1.7%; in combination with positive nodes at other sites: 1.7%). In our method, we were able to identify these lymph nodes using a magnified videoscopic view. Furthermore, we were able to make an incision from the EnSeal insertion port to these lymph nodes along the borderline of the left mediastinal pleura; and en bloc resection was performed



easily. Furthermore, our method enabled us to dissect the left main bronchus lymph nodes via a transhiatal approach.

Our results showed that the total operative bleeding was significantly decreased by using LTHA. Furthermore, the duration of thoracic drainage was significantly shortened in the patients treated with LTHA in comparison with the patients treated without LTHA. We consider that one of the reasons for this is that our method enables dissection of the appropriate layer under a magnified videoscopic view; and therefore, damage to the microvessels and lymphatic ducts is avoided. Except in cases involving large T3 tumors in the upper thoracic region, the LTHA provides a good surgical view, which is not provided by laparotomy, and allows the surgeon to take advantage of videoscope assistance, which is useful because the working space in the mediastinum is narrow and deep.

In laparoscopic surgery, the reconstructed organ is sometimes injured. To avoid this, we perform abdominal operations using HALS and have no experience of reconstructed organs suffering intraoperative injuries so far. From the same point of view, many reports have indicated the efficacy of HALS for esophageal cancer.<sup>21–23</sup> We were able to apply this technique to mediastinal operations without any major problems. Although some reports about mediastinoscope-assisted esophagectomy have described the use of a mediastinoscope from the cervical side,<sup>24–26</sup> most esophageal surgeons do not get used to this surgical view, and therefore, they need to master certain skills. On the other hand, our procedure, which is performed via a transhiatal approach, can easily be performed in institutes that use HALS for abdominal esophageal surgery. In our experience, there were no intraoperative respiratory care problems associated with applying 10 mmHg pneumomediastinum pressure. In this procedure, although mechanical compression with the ENDO RETRACT was used to obtain working space in the mediastinum, it had little effect on cardiovascular function, such as on blood pressure, and there were no problems with maintaining general anesthesia. Under gentle mechanical compression, the same laparoscopic view was maintained, even when a pleural injury occurred in the mediastinum. Furthermore, even in cases involving sudden massive bleeding in the mediastinal space, hand assistance makes it possible to directly press and suture the bleeding point by hand. From these points of view, we consider that our procedure, esophagectomy involving the LTHA, can be performed safely in patients with esophageal cancer.

In conclusion, our surgical procedure, LTHA-preceding esophagectomy, drastically shortened the intrathoracic operative time, decreased intraoperative bleeding, and reduced the amount of postoperative thoracic discharge without increasing the risk of major postoperative complications. In addition,

our procedure produced a good surgical view of the posterior and left mediastinum, and en bloc lymph node dissections around these areas were performed safely.

## References

- 1 Whooley B P, Law S, Murthy S C, Alexandrou A, Wong J. Analysis of reduced death and complication rates after esophageal resection. *Ann Surg* 2001; 233: 338–44.
- 2 Law S, Wong K H, Kwok K F, Chu K M, Wong J. Predictive factors for postoperative pulmonary complications and mortality after esophagectomy for cancer. *Ann Surg* 2004; 240: 791–800.
- 3 Ferguson M K, Durkin A E. Preoperative prediction of the risk of pulmonary complications after esophagectomy for cancer. *J Thorac Cardiovasc Surg* 2002; 123: 661–9.
- 4 Osugi H, Takemura M, Lee S *et al.* Thoracoscopic esophagectomy for intrathoracic esophageal cancer. *Ann Thorac Cardiovasc Surg* 2005; 11: 221–7.
- 5 Osugi H, Takemura M, Higashino M, Takada N, Lee S, Kinoshita H. A comparison of video-assisted thoracoscopic oesophagectomy and radical lymph node dissection for squamous cell cancer of the oesophagus with open operation. *Br J Surg* 2003; 90: 108–13.
- 6 Thomson I G, Smithers B M, Gotley D C *et al.* Thoracoscopic-assisted esophagectomy for esophageal cancer: analysis of patterns and prognostic factors for recurrence. *Ann Surg* 2010; 252: 281–91.
- 7 Noshiro H, Iwasaki H, Kobayashi K *et al.* Lymphadenectomy along the left recurrent laryngeal nerve by a minimally invasive esophagectomy in the prone position for thoracic esophageal cancer. *Surg Endosc* 2010; 24: 2965–73.
- 8 Cadière G B, Dapri G, Himpens J, Rajan A. Thoracoscopic esophagectomy in prone position. *Ann Surg Oncol* 2011; 18: 838.
- 9 Shiozaki A, Fujiwara H, Daisuke I, Okamoto K, Komatsu S, Otsuji E. Pneumomediastinum method for esophageal cancer. *Operation* 2011; 65: 1277–80.
- 10 Shiozaki A, Fujiwara H, Murayama Y *et al.* Posterior mediastinal lymph node dissection using the pneumomediastinum method for esophageal cancer. *Esophagus* 2012; 9: 58–64.
- 11 van Lanschot J J, Hop W C, Voormolen M H, van Deelen R A, Blomjous J G, Tilanus H W. Quality of palliation and possible benefit of extra-anatomic reconstruction in recurrent dysphagia after resection of carcinoma of the esophagus. *J Am Coll Surg* 1994; 179: 705–13.
- 12 van Lanschot J J, van Blankenstein M, Oei H Y, Tilanus H W. Randomized comparison of prevertebral and retrosternal gastric tube reconstruction after resection of oesophageal carcinoma. *Br J Surg* 1999; 86: 102–8.
- 13 Sobin L, Gospodarowicz M, Wittekind C, (eds). *TNM Classification of Malignant Tumors*, 7th edn. Hoboken, NJ: John Wiley & Sons, Inc, 2009.
- 14 Ando N, Kato H, Igaki H *et al.* A randomized trial comparing postoperative adjuvant chemotherapy with cisplatin and 5-fluorouracil versus preoperative chemotherapy for localized advanced squamous cell carcinoma of the thoracic esophagus (JCOG9907). *Ann Surg Oncol* 2012; 19: 68–74.
- 15 Charlson M E, Pompei P, Ales K L, MacKenzie C R. A new method of classifying prognostic comorbidity in longitudinal studies: development and validation. *J Chronic Dis* 1987; 40: 373–83.
- 16 DePaula A L, Hashiba K, Ferreira E A, de Paula R A, Grecco E. Laparoscopic transhiatal esophagectomy with esophagogastric anastomosis. *Surg Laparosc Endosc* 1995; 5: 1–5.
- 17 Bonavina L, Bona D, Binyom P R, Peracchia A. A laparoscopic-assisted surgical approach to esophageal carcinoma. *J Surg Res* 2004; 117: 52–7.
- 18 Montenovolo M I, Chambers K, Pellegrini C A, Oelschlager B K. Outcomes of laparoscopic-assisted transhiatal esophagectomy for adenocarcinoma of the esophagus and esophago-gastric junction. *Dis Esophagus* 2011; 24: 430–6.
- 19 Zingg U, Forberger J, Frey D M *et al.* Inflammatory response in ventilated left and collapsed right lungs, serum and pleural

- fluid, in transthoracic esophagectomy for cancer. *Eur Cytokine Netw* 2010; 21: 50–7.
- 20 De Conno E, Steurer M P, Wittlinger M *et al*. Anesthetic-induced improvement of the inflammatory response to one-lung ventilation. *Anesthesiology* 2009; 110: 1316–26.
- 21 Martin D J, Bessel J R, Chew A, Watson D I. Thoracoscopic and laparoscopic esophagectomy: initial experience and outcomes. *Surg Endosc* 2005; 19: 1597–601.
- 22 Bernabe K Q, Bolton J S, Richardson W S. Laparoscopic hand-assisted versus open transhiatal esophagectomy: a case-control study. *Surg Endosc* 2005; 19: 334–7.
- 23 Glasgow R E, Swanstrom L L. Hand-assisted gastroesophageal surgery. *Semin Laparosc Surg* 2001; 8: 135–44.
- 24 Tangoku A, Yoshino S, Abe T *et al*. Mediastinoscope-assisted transhiatal esophagectomy for esophageal cancer. *Surg Endosc* 2004; 18: 383–9.
- 25 Parker M, Pfluke J M, Shaddix K K, Asbun H J, Smith C D, Bowers S P. Transcervical videoscopic esophageal dissection in minimally invasive esophagectomy. *Surg Endosc* 2011; 25: 941–2.
- 26 Ikeda Y, Niimi M, Kan S, Takami H, Kodaira S. Thoracoscopic esophagectomy combined with mediastinoscopy via the neck. *Ann Thorac Surg* 2002; 73: 1329–31.

## Clinical Impact of Predicting CCND1 Amplification Using Plasma DNA in Superficial Esophageal Squamous Cell Carcinoma

Shuhei Komatsu · Daisuke Ichikawa · Shoji Hirajima · Hiroki Takeshita · Atsushi Shiozaki · Hitoshi Fujiwara · Tsutomu Kawaguchi · Mahito Miyamae · Hiroataka Konishi · Takeshi Kubota · Kazuma Okamoto · Nobuaki Yagi · Eigo Otsuji

Received: 8 May 2013 / Accepted: 17 December 2013 / Published online: 24 January 2014  
© Springer Science+Business Media New York 2014

### Abstract

**Background** This study was designed to evaluate the clinical benefit of predicting the cyclin D1 (CCND1) status using cell-free plasma DNA in superficial esophageal squamous cell carcinoma (ESCC) patients.

**Methods** The ratio of the CCND1 (11q13) dosage to the DRD2 (11q22–23) dosage (C/D-ratio) as the CCND1 copy number was evaluated. This study was divided into three steps: (1) demonstration of the feasibility, (2) evaluation of whether the plasma C/D ratio assay could monitor tumor dynamics, and (3) a validation study in 63 consecutive superficial ESCC (pTis–T1) patients and 40 healthy volunteers.

**Results** (1) The plasma C/D ratio was significantly higher ( $p = 0.0369$ ) in superficial ESCC patients than in the controls in a preliminary test. (2) The high plasma C/D ratio appeared to reflect the tumor levels of the CCND1 status and was reduced in postoperative plasma samples ( $p = 0.1154$ ) and samples following endoscopic resection ( $p = 0.0845$ ).

(3) Validation analysis revealed that the plasma C/D ratio was significantly higher in superficial ESCC patients than in controls ( $p < 0.0001$ ). The frequency of recurrence was significantly higher ( $p = 0.0198$ ), and recurrence-free survival was significantly shorter ( $p = 0.0075$ ) in patients with a high plasma C/D ratio. Moreover, a high C/D ratio was shown to be an independent risk factor for recurrence on multivariate analysis [ $p = 0.0334$ ; odds ratio 10.58 (range 1.203–93.23)].

**Conclusion** The prediction of CCND1 amplification by plasma DNA may be a new complementary clinical biomarker for recurrence in patients with superficial ESCC.

**Keywords** Biomarker · Plasma · Copy number · Cyclin D1 · Superficial esophageal cancer · Amplification · Liquid biopsy

**Electronic supplementary material** The online version of this article (doi:10.1007/s10620-013-3005-2) contains supplementary material, which is available to authorized users.

S. Komatsu (✉) · D. Ichikawa (✉) · S. Hirajima · H. Takeshita · A. Shiozaki · H. Fujiwara · T. Kawaguchi · M. Miyamae · H. Konishi · T. Kubota · K. Okamoto · E. Otsuji  
Division of Digestive Surgery, Department of Surgery, Kyoto Prefectural University of Medicine, 465 Kajii-cho, Kawaramachihirokoji, Kamigyo-ku, Kyoto 602-8566, Japan  
e-mail: skomatsu@koto.kpu-m.ac.jp

D. Ichikawa  
e-mail: ichikawa@koto.kpu-m.ac.jp

N. Yagi  
Department of Molecular Gastroenterology and Hepatology, Kyoto Prefectural University of Medicine, 465 Kajii-cho, Kawaramachihirokoji, Kamigyo-ku, Kyoto, Japan

### Introduction

Esophageal cancer is the eighth most common cancer in the world and the sixth leading cause of cancer mortality [1]. Although esophageal cancer presents as two different kinds of histological types and occurs worldwide with a variable geographic distribution, esophageal squamous cell carcinoma (ESCC) accounts for ~90 % of all esophageal cancer diagnosed in Asian countries [2] and remains one of the most aggressive carcinomas of the gastrointestinal tract because of local invasiveness and metastases in early stage of the clinical course.

Although recent improvements in perioperative management and surgical techniques have reduced surgery-related deaths and improved postoperative outcomes by multidisciplinary approaches [1, 3], the survival rates of patients with advanced ESCC, which invades more than the

muscularis propria, are still very poor. In contrast, patients with superficial ESCC, which invades the mucosa or submucosa, have better prognoses, and most can be curatively treated with radical surgery or at least be treated with endoscopic resection [4, 5]. Nevertheless, recurrence has been reported in some patients even at an early stage. Therefore, predicting recurrence at an early stage and diagnosing residual tumors when they are still minimal or clinically occult may improve the survival rates of patients with ESCC.

Previous studies have attempted to determine which biological factors, such as p53, cyclin D1, and FAS, are involved in tumorigenesis and the development of ESCC [6–9] because identifying molecular targets for the treatment of ESCC may help to improve the survival of these patients. However, few molecules have been used as therapeutic and/or diagnostic biomarkers in a clinical setting. Although conventional serum tumor markers, such as carcinoembryonic antigen (CEA) and squamous cell carcinoma antigen (SCC), have been used in convenient diagnostic assays [10, 11] for the early detection of tumors and monitoring of tumor dynamics in patients with ESCC, they lack sufficient sensitivity and specificity to facilitate the detection of cancer. Therefore, the significance of detecting a novel biomarker using molecules should be emphasized.

Recent studies reported that tumor-released circulating DNA and RNA in plasma/serum samples were useful for detecting tumor-specific abnormalities and monitoring the disease status of cancers [12–16]. Therefore, we hypothesized that genomic amplification could be predicted in primary ESCC using a blood-based test because gene amplification is one of the most frequent genomic aberrations involved in the pathogenesis of ESCC. We previously demonstrated that the genome status of CCND1 in patients with primary esophageal cancer could be predicted by a less invasive, blood-based test, which enabled primary tumor dynamics to be evaluated and the prognosis of patients and its associated clinicopathological factors to be predicted [17]. To avoid the influences of the quantity of plasma DNA and numerical chromosomal aberrations, we invented and specifically calculated the ratio of the dosage of CCND1 to that of the reference single copy gene, dopamine receptor D2 (DRD2) mapped to 11q22–23, as an indicator of the CCND1 copy number (CCND1/DRD2: C/D ratio) [18].

We clearly demonstrated in the present study that measuring the plasma C/D ratio may be clinically beneficial for detecting cancer preoperatively and the resection status by surgery and endoscopy even in patients with superficial ESCC. We also validated its ability to predict recurrence even in patients with superficial ESCC by analyzing the relationship between plasma results and clinicopathological factors. Our findings indicate that

evaluating CCND1 amplification by plasma DNA may serve as a clinical biomarker for superficial ESCC.

## Materials and Methods

### Patients and Samples

This study was approved by the Institutional Review Board of Kyoto Prefectural University of Medicine and each subject provided signed informed consent. Sixty-three consecutive patients with superficial ESCC underwent R0 (no residual tumor after surgery) esophagectomy at the Kyoto Prefectural University of Medicine between 2005 and 2011. A total of 7 ml of peripheral blood was obtained from each patient before surgery and from 40 healthy volunteer controls. Resected cancer specimens from surgery and endoscopic resection were fixed in buffered formalin and embedded in paraffin for a routine pathological examination. The tumor was pathologically classified according to the UICC classification [19].

### Preparation and DNA Isolation of Plasma and Tissue Samples

Following the collection of peripheral blood, cell-free nucleic acids were immediately isolated from blood samples by the 3-spin protocol (1,500 rpm for 30 min, 3,000 rpm for 5 min, 4,500 rpm for 5 min) to prevent cross contamination from cellular nucleic acids [20]. Following centrifugation, plasma samples were stored at  $-80^{\circ}\text{C}$  until further processing. Cell-free genomic DNA was isolated from 400  $\mu\text{l}$  of the serum sample using the QIAamp blood mini kit (Qiagen, Hilden, Germany). The final elution was performed in 100  $\mu\text{l}$  of AE buffer from the QIAamp blood mini kit. Paraffin-embedded tissues were sectioned at a thickness of 5  $\mu\text{m}$  after a routine histological examination. The genomic DNAs of cancerous and adjacent noncancerous esophageal tissues were extracted from two 5- $\mu\text{m}$  thick slices using DEXPAT (TaKaRa, Kyoto, Japan) according to the manufacturer's protocols.

### Quantitative Analysis for Cyclin D1 Using Real-Time Polymerase Chain Reaction (PCR)

We selected the dopamine-D2-receptor gene (DRD2) as a reference gene because DRD2 is located on the same chromosome as CCND1, and DRD2 amplification and overexpression in ESCC have never been reported in any gene database, such as GenBank, DDBJ, and EMBL. Therefore, the CCND1/DRD2 ratio may reflect the CCND1 copy number at a single chromosome without the influence of absolute DNA concentration and aneuploidy on chromosome 11